Electronic Supplementary Information

In-situ real-time neutron imaging of gaseous H$_2$ adsorption and D$_2$ exchange on carbon-supported Pd catalysts

Hamish Cavaye,[a] Christos Ballas,[b] Winfried Kockelmann,[a] David Lennon,[b] Paul Collier,[c] Andrew P. E. York,[c] Peter W. Albers,[d] Stewart F. Parker[a,b]

a)   ISIS Pulsed Neutron and Muon Source, STFC Rutherford Appleton Laboratory
Chilton, OX11 0QX, UK. E-mail: stewart.parker@stfc.ac.uk.
b)   School of Chemistry, University of Glasgow, Joseph Black Building, Glasgow G12 8QQ, UK.
c)   Johnson Matthey Technology Centre, Blounts Court, Sonning Common, Reading RG4 9NH, UK.
d)   Evonik Technology & Infrastructure GmbH, Rodenbacher Chaussee 4, 63457 Hanau-Wolfgang, Germany.
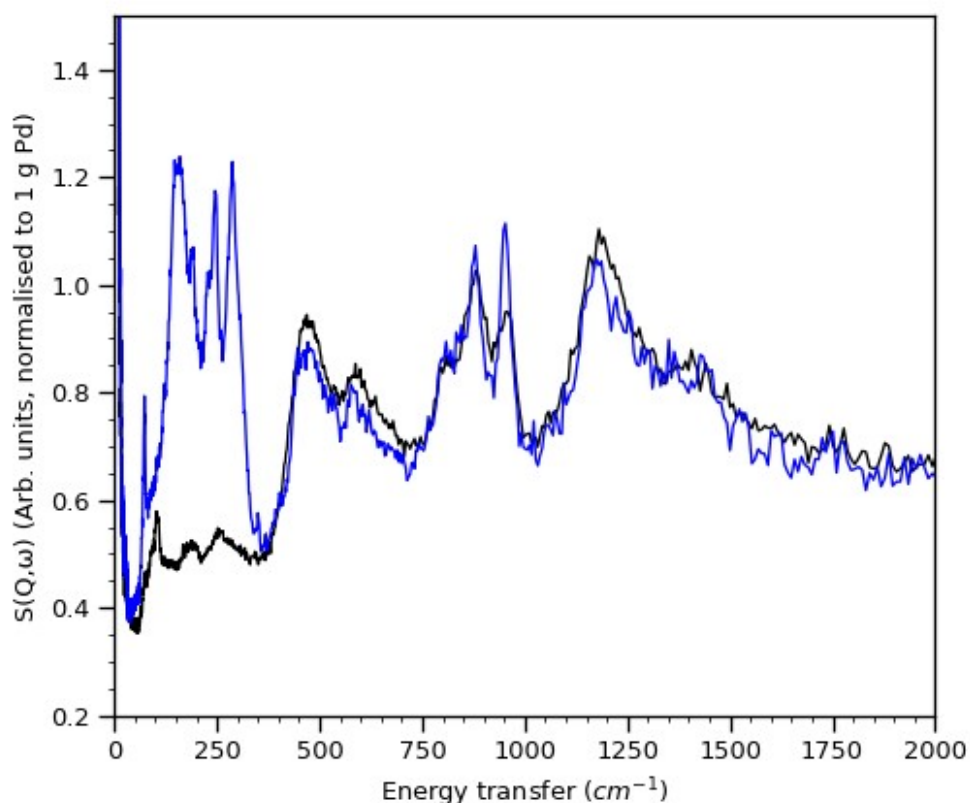
Table of Contents

Figure S1. Inelastic neutron scattering (INS) spectra of Sample 2 (black line) and a sample of verified H_2 adsorbed on a Pd/C catalyst (blue line).[1] The intense features below ~400 cm^{-1} are due to the aluminium sample can used for the neutron imaging measurements.

Figure S1 shows the INS vibrational spectrum, between 0-2000 cm^{-1}, for Sample 2 after exposure to 20% H_2 in He carrier gas to ensure complete adsorption of H_2 in the catalyst bed in the same manner as during the neutron imaging experiment (main manuscript Figure 2). The spectrum is compared to a verified sample of H_2 adsorbed on a larger sample of the same 20 wt% Pd/C catalyst after exposure to 700 mbar atmosphere of H_2, as previously reported by Parker *et al.*;[1] both spectra are normalised to ~1 g of total Pd content. The bands centred around 1200 cm^{-1} and 800 cm^{-1} are from the carbon support and the three peaks below 300 cm^{-1} are caused by the aluminium sample cans. The bands around 450-700 cm^{-1} are the signal from β-palladium hydride (β-PdH$_x$).

Materials and methods

The Pd(20 wt%)/C sample was the same as that used previously.[1] This was prepared by Evonik Industries by wet impregnation of a powder type high surface area activated carbon, (nitrogen surface area > 1000 m^2/g, steam activated, total pore volume > 1.3 ml g^{-1}, hydrogen content 3900 ppm H). Table S1 lists the analytical data for this material and Figure S1 shows a TEM image and the derived particle size distribution. The Pd(5 wt%)/C catalyst: Pd 4.8 wt% on activated carbon (nitrogen surface area 1050 m^2/g) was supplied by Aldrich (Sigma Aldrich Cat. No. 205680).

Table S1 Results of statistical evaluations of the TEM images and the XPS signal region, of the precious metals.

Catalyst sample	DN / nm	S_{DN} / nm	DA / nm	EMS / m^2g^{-1}	XPS / at.%
Pd(20%)/C	3.58	2.21	7.44	67.20	15.3

TEM: DN and S_{DN} : primary particle size (arithmetical average) and its standard deviation; DN=$(\Sigma n_i d_i)$/N; DA: primary particle size averaged over the surface, DA=$(\Sigma n_i d_i^3)$ /$(\Sigma n_i d_i^2)$; EMS: calculated electron microscopic surface, EMS= 6000/(DA × ρ); ρ_{Pd} = 12.02 g cm^{-3};
XPS: signal contribution of already nearly reduced precious metal species to the whole XPS-signal group, measured in the topmost atomic layers of the freshly impregnated and, for the calcined catalysts and the alloy catalyst, prior to the subsequent in-situ hydrogenation cycles. Adapted from reference [1] under an Attribution 3.0 Unported (CC BY 3.0) license.
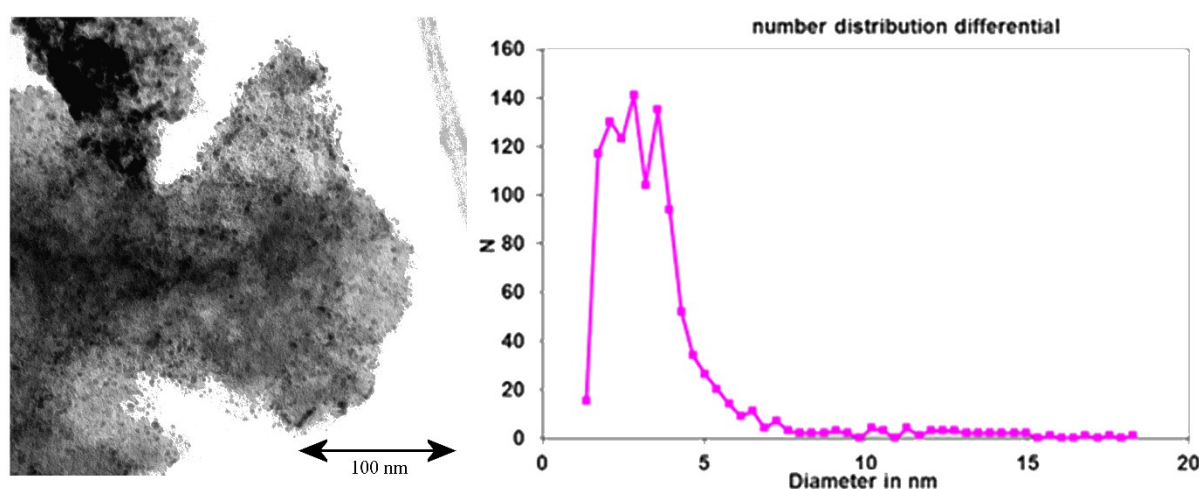

Figure S2. Left: TEM image of the Pd(20 wt%)/C catalyst (mostly isolated primary particles on/in the porous high surface area activated carbon support). Right: TEM size distribution of the Pd(20 wt%)/C catalyst determined by evaluation of > 1000 isolated as well as aggregated primary particles per sample. Adapted from reference [1] under an Attribution 3.0 Unported (CC BY 3.0) license.

Samples 1 and 2 were reduced in hydrogen in an Inconel cell that has been described previously,[5] before transfer in a glove box into flat plate aluminium cells. (The transfer was required because the temperature needed to decompose the β-PdH_x (200 °C) is above the operating limit of the Al cells). Sample 3 was loaded into a flat plate stainless steel.[5] Sample 3 was reduced in the cell without the need to transfer it because of the higher operating temperature of the cell.

Neutron radiography (NR)

Neutron radiography was performed at the IMAT beamline[2] of the ISIS neutron spallation source, Rutherford Appleton Laboratory, UK, using a polychromatic neutron beam of wavelength range 0.7 - 6.7 Å. A sample cell was mounted 43 mm in front of a ZnS/^{6}LiF scintillator screen (100 µm thickness) of a neutron camera. The scintillator was coupled via a 45° mirror and a focussing lens of 105 mm focal length to a CCD camera (ANDOR IKON-L, Oxford Instruments, UK) with 2048 × 2048 pixels, providing a field-of-view of 99.3 x 99.3 mm^2 and a pixel size of 48.4 x 48.4 µm^2. The camera was at a distance L = 10.4 m from a beam aperture (pinhole) of diameter D. A beam aperture of D = 100 mm defined an L/D ratio of 100, providing a geometric blur and a resolution limit of about 430 µm. Radiograms were recorded with an exposure time of 5 s every 9 s. Stacks of 50 open-beam (no sample) and 20 dark images (neutron source off) were collected for normalisation (flat-fielding) purposes.

Image processing methods

Raw frames were processed in Mantid Imaging (ver. 2.6.0a1.post19).[3] Bright and dark outlier pixels were removed and replaced by a kernel size = 3 average value from surrounding pixels. Each dataset also underwent region of interest (ROI) normalisation, in which the average brightness of a chosen air/direct beam region of the frames was set to be equal, correcting for small and short-term fluctuations in neutron beam flux. Each frame was flat-fielded using open beam and dark frames.

Analysis of the image data was undertaken using python scripts written specifically for purpose. ROIs were selected to cover a range of different parts of each sample. The average grey values for these samples were calculated for each frame and in order to allow comparison between regions with different absolute grey values, the data were then normalised to the first 50 frames. Lastly, to aid the visual interpretation of these resulting grey value curves, a Savitzky-Golay filter[4] (window length 71, polynomial order 3) was applied. Both the unsmoothed and filtered data are presented below (Figures S3 and S4).
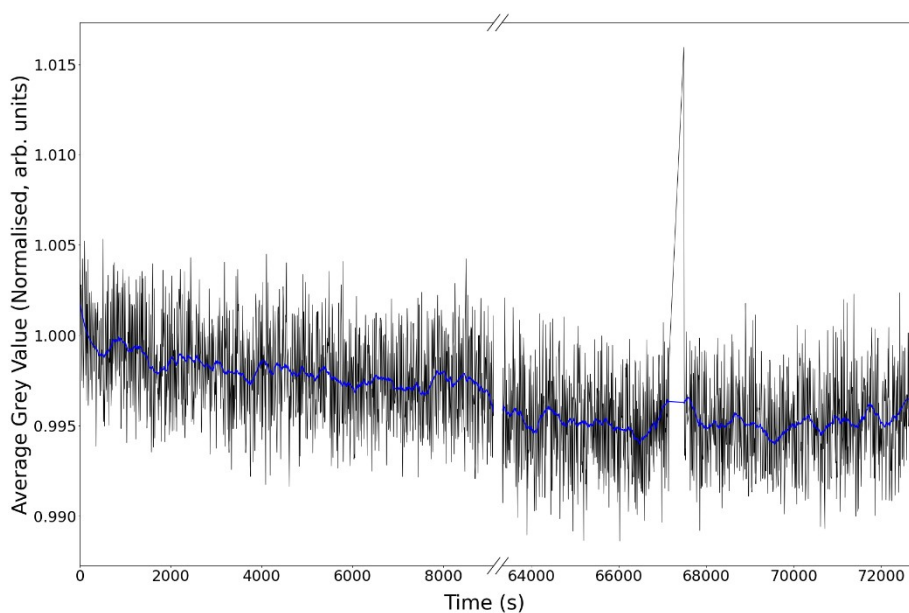
Sample 1

Figure S3. Representative average grey value in the region of interest denoted by a black square in main manuscript Figure 2 (quartz wool region). Shown are the raw data (black line) and the data after smoothing with a Savitzky–Golay filter (blue line). Note that the filter has removed a peak at about 67500 s, caused by an imperfect correction of a neutron source trip.
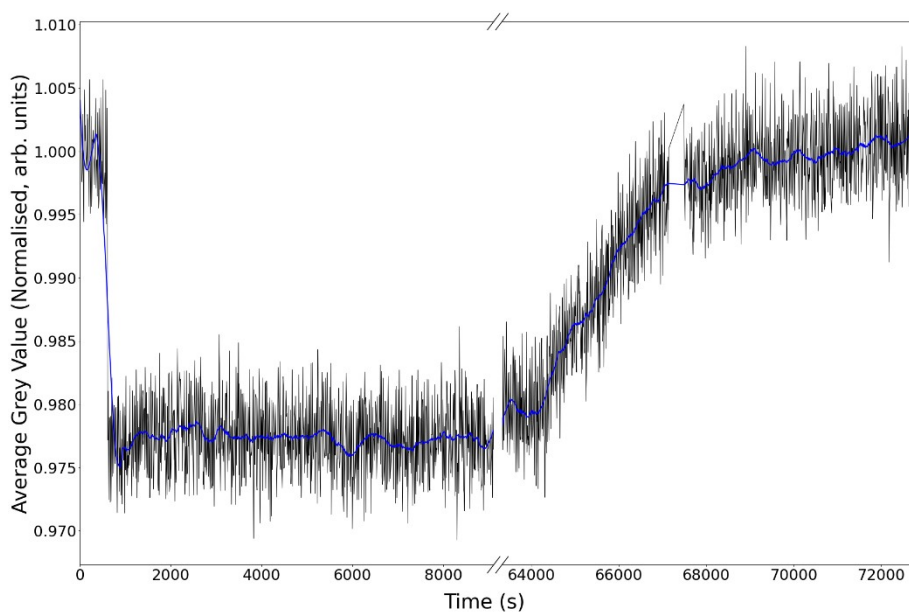

Figure S4. Representative average grey value in the region of interest denoted by a blue square in main manuscript Figure 2 (within the catalyst bed, lower region, near gas in-flow). Shown are the raw data (black line) and the data after smoothing with a Savitzky–Golay filter (blue line). The break in the raw data at about 67500 s is due to a neutron source outage, lasting a few minutes.

Supplementary video of Sample 1*:* Time-sequence of 200 radiographs for catalyst bed of Sample 1 over a period of 1548 s (~26 mins) that visualises the advancing front of hydrogen absorption through the catalyst bed. Selected radiographs are displayed in Figure 3 of the main manuscript. A reference radiograph, recorded before H_2 gas dosing, was subtracted from each image of the H_2 adsorption experiment. The images were cropped to 520 x 520 pixels; the time difference between radiographs is 9 s. This produced a set of "difference images", highlighting just regions of the data that changed over time. A strong feature on the left-hand side, caused by an initial shift in the position of some of the catalyst powder upon gas flow initiation, can be ignored for the purposes of examining H_2 adsorption.

[H2_Diffusion_Video.avi: link to be provided by RSC]

Sample 2

Figure S5. Full frame neutron radiograph of Sample 2 in a stainless steel cell. This image comprises 250 seconds of total exposure, created by averaging 50 × 5s-radiographs for reduced noise levels. Coloured squares correspond to regions of interest (ROI), the time evolution of these is plotted in Figure S6.
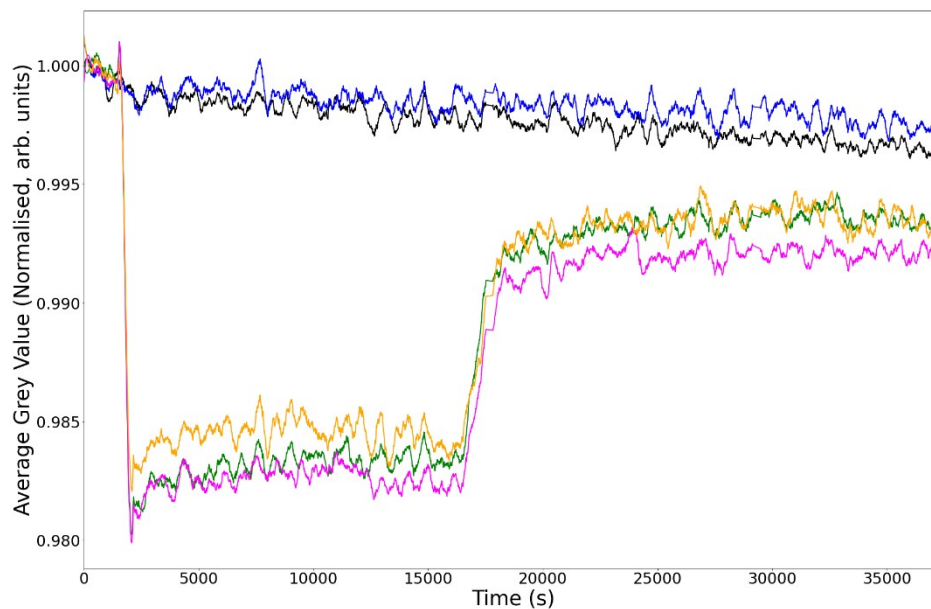

Figure S6. Average grey values for each ROI in Figure S3, with corresponding colours. The data are normalised such that the first 50 frames have an average value of 1. The curves have been Savitzky–Golay filtered to reduce the noise.

References

1. S.F. Parker, H.C. Walker, S.K. Callear, E. Grünewald, T. Petzold, D. Wolf, K. Möbus, J. Adam, S.D. Wieland, M. Jiménez-Ruiz and P.W. Albers, The effect of particle size, morphology and support on the formation of palladium hydride in commercial catalysts, *Chemical Science* 10 (2019) 480-489, DOI: 10.1039/C8SC03766C.
2. T. Minniti, K. Watanabe, G. Burca, D.E. Pooley, W. Kockelmann, Characterization of the new neutron imaging and materials science facility IMAT, *Nucl. Instrum. Methods Phys. Res. Sect. A* 888 (2018) 184–195, DOI: /10.1016/j. nima.2018.01.037.
3. S Tygier, D Akello-Egwel, J Allen, R Baust, J Bradley, G Burca, A Fedrigo, M Gigg, S Jones, W Kockelmann, D Nixon, D E Pooley and D Tasev. Tomographic reconstruction with Mantid Imaging. Proceedings of 9th International Topical Meeting on Neutron Radiography 17-21 Oct 2022 in Buenos Aires, *J. Phys. Conf. Ser.*, accepted for publication.
4. A Savitzky and M. J. E. Golay, Smoothing and Differentiation of Data by Simplified Least Squares Procedures. *Analytical Chemistry* 1964 36 (8), 1627-1639, DOI: 10.1021/ac60214a047.
5. R. Warringham, D. Bellaire, S. F. Parker, J. Taylor, C. M. Goodway, M. Kibble, S. R. Wakefield, M. Jura, M. P. Dudman, R. P. Tooze, P. B. Webb and D. Lennon, Sample environment issues relevant to the acquisition of inelastic neutron scattering measurements of heterogeneous catalyst samples, *J. Phys. Conf. Ser.*, 2014, **554**, 012005.